Sedimentary processes and Quaternary stratigraphy of the Old Harry area, Gulf of St. Lawrence

Naïs Sirdeys[1*], Guillaume St-Onge[1], Jean-Carlos Montero-Serrano[1], Noela Sànchez-Carnero[2], Pierre-Arnaud Desiage[1]

[1]Institut des sciences de la mer de Rimouski, Canada Research Chair in Marine Geology, Université du Québec à Rimouski et GEOTOP, 310 allée des Ursulines, Rimouski, Québec, G5L 3A1, Canada

[2]Centro para el Estudio de Sistemas Marinos (CESIMAR-CCT CONICET-CENPAT),Boulevard Brown 2915, Puerto Madryn, Argentina

* naissirdeys@outlook.fr

Arctic Change 2017

Introduction

The Old Harry (OH) offshore oil and gas prospect is a geological structure subject to numerous estimates of its volume, extractable quantities, and environmental hazards associated with its possible exploitation, but remains scarcely documented.

In this context, we present here a multi-proxy record, including geophysics, sedimentological, geochemical, geochronological (^{14}C) and paleomagnetic analyses (inclination, declination and relative paleointensity), in order to: (1) to improve the geological characterization of this area since the last glaciation, and (2) reconstruct of post-glacial evolution of sedimentary environments and processes.

The 13 box and piston cores retrieved in 2015 on board the R/V Coriolis II will help establishing a chronostratigraphic framework of this formerly glaciated continental margin. The 1300 km of geophysical data and 230 km^2 of multibeam coverage highlighting the bathymetry, as well as the presence of more than 3000 pockmarks[4] were collected in the same time and will be integrated here.

Methodology

Seismic

Acquisition of data with an Edgetech X-Star 2.1 Chirp (4.5-6 kHz) → Conversion in SEG-Y format using discover X-star → Swell correction and seafloor reflection picking → **Processing amplitude correction and signal to noise ratio improvement** → **Definition of seismic attributes** (Hilbert) for data interpretation → **Tide correction** using a MATLAB function

Sub-sampling at laboratory (ISMER) (photo by Sarah Letaïef)

13 cores

- 4 piston cores
- 4 gravity cores
- 5 box cores

- **CT-scan**
- **MSCL analysis** (density, magnetic susceptibility, P-wave velocity, diffuse spectral reflectance) « whole/split »
- **Digital imaging**
- **Visual description**
- **U-channels** (~ 20 m)
  - **Geochemistry** (XRF core scanner)
  - **Cryogenic magnetometer**
- **Sub-samples** (n~ 300)
  - **Magnetic mineralogy and grain-size (AGM)**
  - **Stable isotopes** δ^{13}C and δ^{15}N
  - **Grain-size**
- **Shells and organic matter sampling** (^{14}C dating)
  - **Age model** (chronostratigraphy)

Mutlibeam data acquisition
(Kongsberg Maritime EM 302 and 2040 multibeam echosuonders) integrated in real time (Kongsberg SIS software)

Corrections on *CARIS*
(sound velocity with depth, tide)

Bathymetry

Identification of *pockmarks*
(ArcGIS)

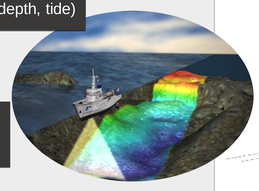

Fig. 1. Image of multibeam acquisition (*from www.nauticalcharts.noaa.gov*)

Location of the study area

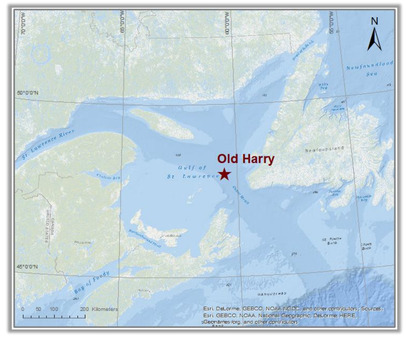

Fig. 2. Bathymetric map of the Gulf of St. Lawrence with the Laurentian Channel and the position of the Old Harry prospect site (brown star).

Fig. 3. Bathymetric map of the Old Harry area illustrating the location of the cores and the seismic lines

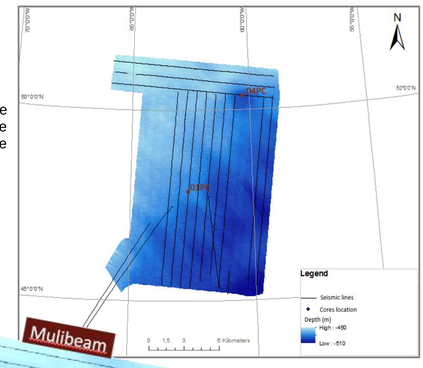

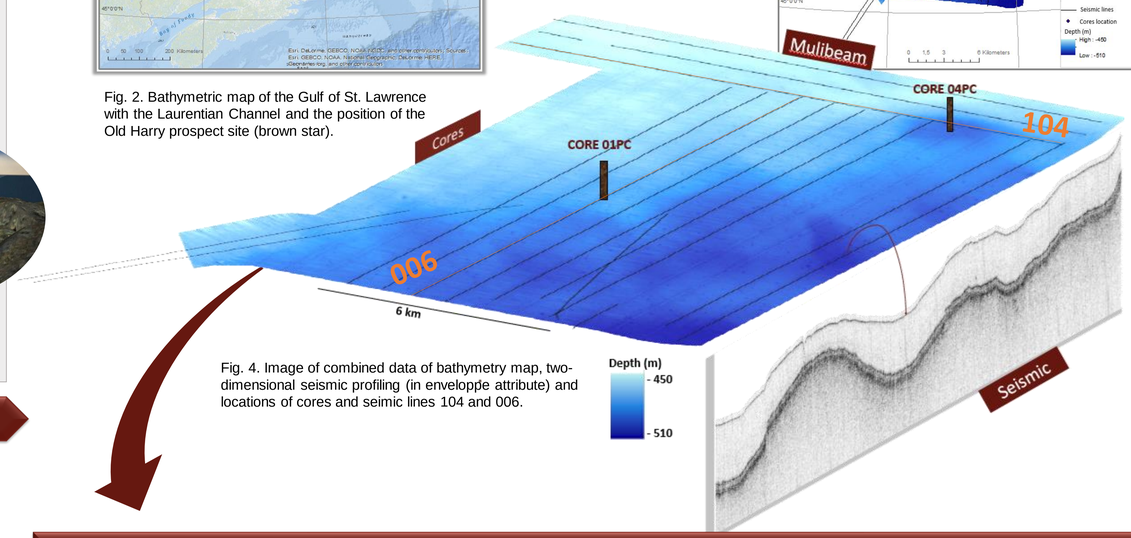

Fig. 4. Image of combined data of bathymetry map, two-dimensional seismic profiling (in enveloppe attribute) and locations of cores and seimic lines 104 and 006.

Seismostratigraphy

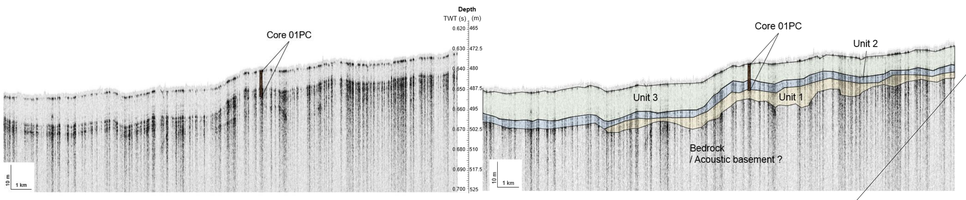

Fig. 5. Data before (left) and after (right) the data processing and interpretations (envelope attribute) procedure (chirp line 006; TWT: Two-Way time) with the location of core 01PC.

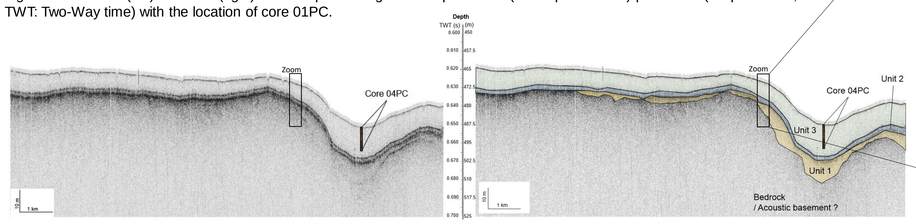

Fig. 6. Data before (left) and after (right) the data processing and interpretations (envelope attribute) procedure (chirp line 104; TWT: Two-Way time) with the location of core 04PC.

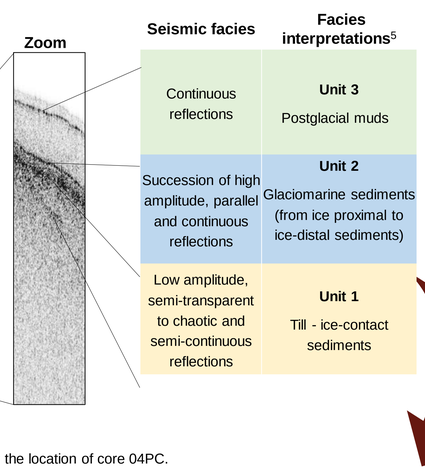

Seismic facies	Facies interpretations[5]
Continuous reflections	**Unit 3** Postglacial muds
Succession of high amplitude, parallel and continuous reflections	**Unit 2** Glaciomarine sediments (from ice proximal to ice-distal sediments)
Low amplitude, semi-transparent to chaotic and semi-continuous reflections	**Unit 1** Till - ice-contact sediments

Bathymetric features : pockmarks

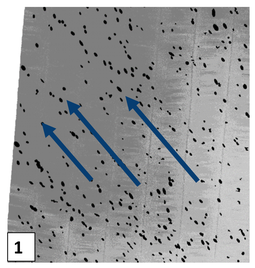

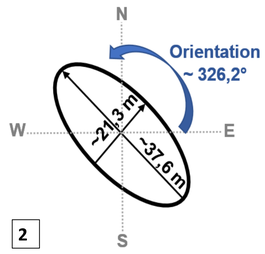

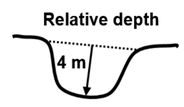

1 2 3

Fig. 10. Left to right: 1. Bathymetry and pockmarks where arrows indicate their alignment. 2. Average length of the major and minor axes with the average orientation. 3. Mean relative depth.

Features

→ **8.1 m < Diameter < 166.8 m**

→ **50.3 m < Perimeter < 771.4 m**

→ **0.7 m < Relative depth < 11.3 m**

Most of the pockmarks are ellipsoids with 326.2° N-W preferential orientation. 21.3 m and 37.6 m are respectively the average length of the minor and major axes.

Isopachs of the Quaternary deposits

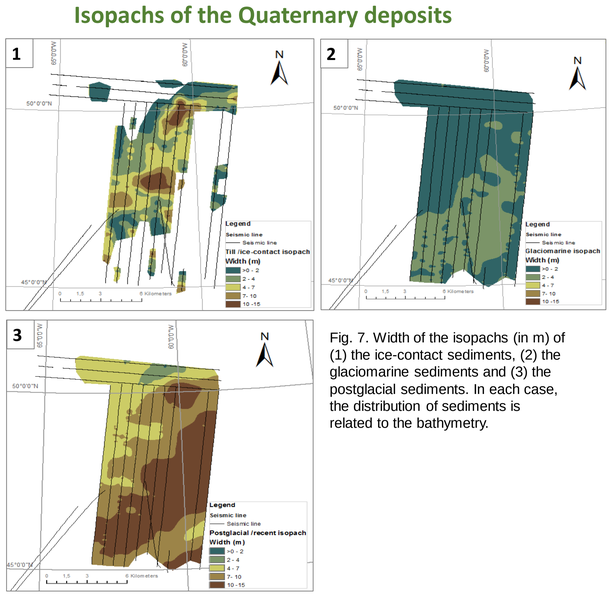

Fig. 7. Width of the isopachs (in m) of (1) the ice-contact sediments, (2) the glaciomarine sediments and (3) the postglacial sediments. In each case, the distribution of sediments is related to the bathymetry.

Evolution of the sedimentation

Lithostratigraphy of the cores

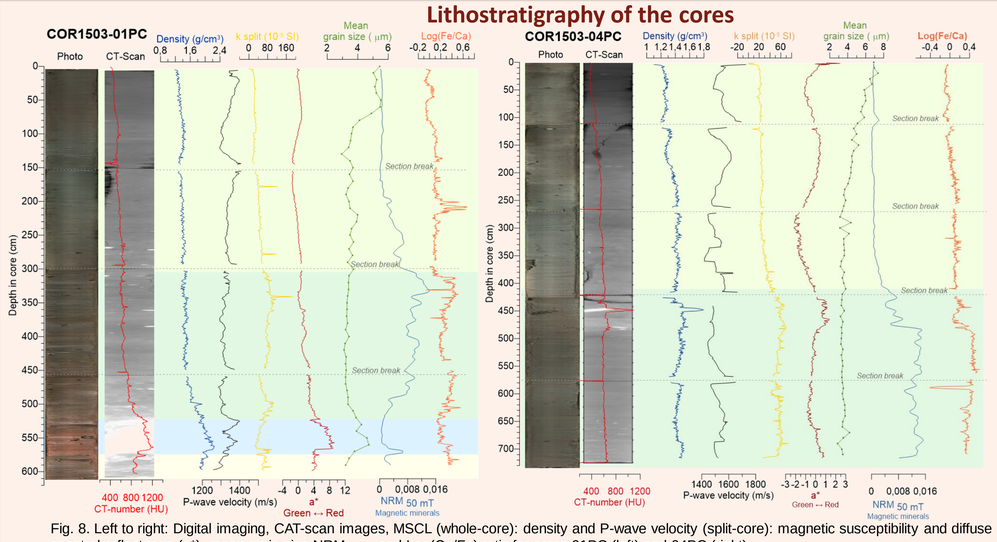

Fig. 8. Left to right: Digital imaging, CAT-scan images, MSCL (whole-core): density and P-wave velocity (split-core): magnetic susceptibility and diffuse spectral reflectance (a*), mean grain size NRM $_{50\ mT}$ and Log(Ca/Fe) ratio for cores 01PC (left) and 04PC (right).

Age-depth model

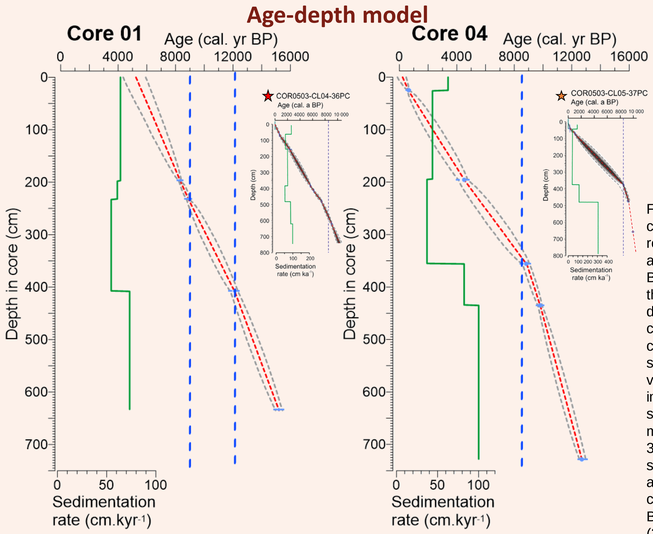

Fig. 9. Age models for composite cores 01 and 04. The age–depth relationship was built with a Bayesian approach using the R-package Bacon[2]. The red dashed line shows the best age model and the grey dashed lines represents the chronological uncertainties (95% confidence interval) with their sedimentation rates in green. The vertical blue dashed lines depict the important changes in the sedimentation rates. Age-depth models for cores COR0503-CL04-36PC[1,3] and COR0503-CL05-37PC[1,3] shows similarities respectively with 01 and 04. In core 04 an important change is observed around 8.5 cal. ka BP as showed by Barletta et al. (2010)[1].

Conclusions

- **230 km^2 of multibeam coverage highlights the bathymetry where 3066 pockmarks were counted (~ 13 pockmarks/km^2). Their NW-SE alignment and orientation could be interpreted as bedrock topography deformations and/or due to the interaction between gas/fluid expulsion and currents[4].**
- **Seismic data present the seismic facies from unit 1 to 3 described by Josenhans and Lehman (1999)[5].**
- **Those seismic facies respectively correspond to ice-contact sediments, glaciomarine sediments and postglacial/modern sediments also found in cores 01 and 04.**
- **In core 04, the age-depth models indicate different sedimentation rates before (90 cm/ka) and after (40 cm/ka) 8.5k cal a BP[1, 3].**
- **Isopach maps demonstrate the distribution of the different seismic units.**

References

[1] Barletta, F., St-Onge, G., Stoner, J.S., Lajeunesse, P., Locat, J., 2010. A high-resolution Holocene paleomagnetic secular variation and relative paleointensity stack from eastern Canada. Earth Planet. Sci. Lett. 298, 162–174.

[2] Blaauw, M. & Christen, J. A. 2011: Flexible paleoclimate age-depth models using an autoregressive gamma process. Bayesian Analysis 6, 457–474.

[3] Casse, M., Montero-Serrano, J.-C., St-Onge, G., 2017. Influence of the Laurentide Ice Sheet and relative sea-level changes on sediment dynamics in the Estuary and Gulf of St. Lawrence since the last deglaciation. Boreas 46, 541–561.

[4] Hovland, M., Judd, A.G., 1988. Seabed pockmarks and seepages impact on the geology, biology and the marine environment. Graham and Trotman Limited, London.

[5] Josenhans, H., Lehman, S., 1999. Late glacial stratigraphy and history of the Gulf of St. Lawrence, Canada. Can. J. Earth Sci. 36, 1327–1345.

[6] Schattner, U., Lazar, M., Souza, L.A.P., Ten Brink, U., Mahiques, M.M., 2016. Pockmark asymmetry and seafloor currents in the Santos Basin offshore Brazil. Geo-Marine Lett. 1–8.

Acknowledgements

We sincerely thank the captain, crew and scientific participants of the COR1503 expedition on board the R/V Coriolis II. The authors are also thankful to Marie-Pier St-Onge and Quentin Beauvais for their help in the laboratory at ISMER and to Melany Belzile for the tide correction algorithm. Financial support for this research was provided by CRSNG Discovery and Ship Time grants to G. St-Onge and J.-C. Montero-Serrano. The use of the VISTA Desktop Seismic Data Processing and Kingdom Suite® software was made possible by Schlumberger and IHS through university partnership programs.